ARTICLE
Journal of Cellular Biochemistry 116:1431–1441 (2015)

Journal of Cellular Biochemistry

iTRAQ-Based Quantitative Proteomic Analysis of Nasopharyngeal Carcinoma

Xin-Zhang Cai,[1] Wei-Qun Zeng,[2,3] Yi Xiang,[3] Yi Liu,[3] Hong-Min Zhang,[3] Hong Li,[3] Sha She,[3] Min Yang,[3] Kun Xia,[1*] and Shi-Fang Peng[4,5**]

[1]*State Key Laboratory of Medical Genetics, Central South University, Changsha, Hunan, China*

[2]*Department of Infectious Diseases, The Second Affiliated Hospital, Chongqing Medical University, Chongqing, China*

[3]*Key Laboratory of Molecular Biology for Infectious Diseases, Ministry of Education, The Second Affiliated Hospital, Chongqing Medical University, Chongqing, China*

[4]*Department of Hepatology and Infectious Diseases, Xiangya Hospital, Central South University, Changsha, Hunan, China*

[5]*Department of Health Management Center, Xiangya Hospital, Central South University, Changsha, Hunan, China*

ABSTRACT

Nasopharyngeal carcinoma (NPC) is a common disease in the southern provinces of China with a poor prognosis. To better understand the pathogenesis of NPC and identify proteins involved in NPC carcinogenesis, we applied iTRAQ coupled with two-dimensional LC-MS/MS to compare the proteome profiles of NPC tissues and the adjacent non-tumor tissues. We identified 54 proteins with differential expression in NPC and the adjacent non-tumor tissues. The differentially expressed proteins were further determined by RT-PCR and Western blot analysis. In addition, the up-regulation of HSPB1, NPM1 and NCL were determined by immunohistochemistry using tissue microarray. Functionally, we found that siRNA mediated knockdown of NPM1 inhibited the migration and invasion of human NPC CNE1 cell line. In summary, this is the first study on proteome analysis of NPC tissues using an iTRAQ method, and we identified many new differentially expressed proteins which are potential targets for the diagnosis and therapy of NPC. J. Cell. Biochem. 116: 1431–1441, 2015.

KEY WORDS: NASOPHARYNGEAL CARCINOMA; PROTEOME; iTRAQ

Nasopharyngeal carcinoma (NPC) is the most lethal among the head and neck cancers. The morbidity of NPC is high in Asia, especially in the southern provinces of China [Wei and Sham, 2005]. Because NPC is usually diagnosed at advanced stages when either radiotherapy or surgery are no longer options, the prognosis of NPC patients is poor. Unfortunately, NPC is difficult to diagnose early because of its deep primary location, non-specific symptoms and lack of specific biomarkers [Feinmesser et al., 1992]. Therefore, there is urgency to discover biomarkers associated with NPC for early diagnosis of NPC.

Several attempts over the past decades have been made using genetic and proteomic methods to identify novel NPC biomarkers. For example, in a recent study, a CCNE1 rs3218073 polymorphism was proposed as a potential biomarker of NPC [Liu et al., 2013]. Proteomic analysis of the radioresistant NPC cell line CNE2-IR and its parental CNE2 cell line showed that 14-3-3σ, Maspin, GPR78, and Mn-SOD may predict the response of NPC to radiotherapy [Feng et al., 2010]. Other studies [Cao et al., 2011; Yu et al., 2011; Chan et al., 2013] have focused on Epstein–Barr virus (EBV) serological antibodies, since EBV is widely considered to be a high-risk factor for NPC [Yu, 1990]. Unfortunately, the low specificity of the EBV serology assay limits the test as a primary means of detection [Anghel et al., 2012].

In nasopharyngeal carcinoma proteomic studies, a large dynamic protein concentration range is an important factor that obstructs the discovery of biomarkers or drug targets. 2-DE is deficient in linear visualization range, sample capacity, reproducibility, and sensitivity for hydrophobic membrane proteins and low concentration proteins [Gorg et al., 2000, 2004]. Consequently, many potentially valuable biomarker proteins may escape detection in conventional 2-DE approaches because of low-abundance. Over the past decade, isotope-based quantitative proteomics have been increasingly applied in biomarker discovery to overcome the disadvantages of 2-DE. These technologies include the in vivo labeling method called stable isotope

Xin-Zhang Cai and Wei-Qun Zeng contributed equally to this work.

*Correspondence to: Prof. Kun Xia, State Key Laboratory of Medical Genetics, Central South University, Changsha, Hunan, China. E-mail: xiakun@sklmg.edu.cn

**Correspondence to: Dr. Shi-Fang Peng, Department of Hepatology and Infectious Diseases, Xiangya Hospital, Central South University, 87# Xiangya Rd, Changsha, Hunan, China. E-mail: sfp1988@gmail.com

Manuscript Received: 10 February 2014; Manuscript Accepted: 23 January 2015

Accepted manuscript online in Wiley Online Library (wileyonlinelibrary.com): 3 February 2015

DOI 10.1002/jcb.25105 • © 2015 Wiley Periodicals, Inc.

labeling by amino acids in cell culture (SILAC), and the in vitro labeling technique termed isobaric tags for relative and absolute quantitation (iTRAQ) [Mirgorodskaya et al., 2000]. The iTRAQ method could simultaneously analyze as many as eight samples in one single test. Therefore, in this study we applied iTRAQ to compare the proteomic profiles of NPC tissues and the adjacent non-tumor tissues, in order to identify novel candidate biomarkers for NPC diagnosis and treatment.

METHODS

TISSUE SAMPLE AND CELL LINE

This study was approved by the Ethics Committee of the Central South University. Nasopharyngeal carcinoma tissues and the adjacent non-tumor tissue samples (n = 9) were provided by Xiangya Hospital of Central South University (Supplementary Information 1). All tissue samples were collected following informed consent of patients without any therapy, and were histopathologically verified.

A human highly differentiated nasopharyngeal squamous carcinoma cell line (CNE1) was cultured in RPMI-1640 medium supplemented with 10% fetal bovine serum (FBS) and 1% Penicillin–Streptomycin solution in a 5% CO_2–water incubator at 37°C.

REAGENTS

Sequencing grade modified trypsin utilized in the iTRAQ labeling was purchased from Promega (Madison, WI). The iTRAQ® Reagent 8 Plex One Assay kit and the corresponding buffer kit were obtained from Applied Biosystems (Foster City, CA). Monoclonal antibodies against beta-actin, heat shock protein beta-1 (HSPB1), nucleophosmin (NPM1), nucleolin (NCL) and serpin peptidase inhibitor B3 (SCCA1) were purchased from Abcam (Cambridge, MA). Anti-IgG antibodies conjugated with horseradish peroxidase (HRP) were purchased from Santa Cruz Biotechnology (Shanghai, China). Enhanced chemiluminescence (ECL) Western blotting detection reagents were purchased from GE Healthcare (Buckinghamshire, England). Human specific NPM1 small interfering RNA (siRNA) oligonucleotides were purchased from OriGene Technologies (Rockville, MD). Lipofectamine® 2000 transfection reagent was acquired from Invitrogen (Carlsbad, CA). CytoSelect™ 24-Well Cell Migration and Invasion Assays (8 μm, Colorimetric Format) were from Cell Biolabs (San Diego, CA).

iTRAQ LABELING

Total protein samples were extracted from NPC tissues and the adjacent normal tissues using lysis buffer containing 7 M urea, 1 mM PMSF, 1 mM Na_3VO_4 and 1 mg/ml DNase I, and centrifuged at 12,000*g* and 4°C for 30 min. The 2-D Quant Kit (Amersham Biosciences, Uppsala, Sweden) was used to quantify total protein in the supernatants of each sample. Equal amounts of protein samples from NPC tissues and adjacent non-tumor tissues from nine patients were respectively pooled to form two NPC protein samples and two adjacent non-tumor protein samples. One hundred micrograms protein of each sample were precipitated with acetone at −20°C overnight, dissolved in urea triethylammonium bicarbonate buffer, then denatured, and cysteine-blocked according to the iTRAQ protocol provided by Applied Biosystems. Next, the samples were digested with 20 μl trypsin solution (0.1 mg/ml, Promega) at 37°C overnight. Then the two NPC protein samples were labeled with 118 and 121 iTRAQ tags respectively, while two adjacent non-tumor protein samples were labeled with 117 and 119 tags, respectively. For further analysis, all labeled samples were eventually collected in one microcentrifuge tube.

PEPTIDE FRACTIONATION

The iTRAQ-labeled peptide samples were fractionated using isoelectric focusing (IEF) as previously described [Yang et al., 2012]. Briefly, the samples were dissolved in Pharmalyte and urea solution (Amersham Biosciences), subsequently applied on pH 3–10 IPG strips (Amersham Biosciences), and then subjected to focus on IPGphor (Amersham Biosciences). Peptides were extracted from the gel using buffer A (2% acetonitrile and 0.1% formic acid) and lyophilized under vacuum. Next, the fractions were desalinated using a Solid Phase Extraction (SPE) column (Supelco, Bellefonte, PA) and lyophilized again. The fractions were then stored at −20°C.

MASS SPECTROMETRIC ANALYSIS

Mass spectrometric analysis was performed using a QStar® Elite hybrid mass spectrometer (Applied Biosystems) coupled to a liquid chromatography system (Amersham, The Netherlands). Lyophilized samples were resuspended in buffer A, and 10 μl were loaded on a capillary column for peptide separation. Peptides were automatically separated by eluting with buffer A and a series of buffer B (98% acetonitrile containing 0.1% formic) gradients at a 0.3 μl/min flow rate. The LC eluent was applied to the electrospray ionization (ESI) quadrupole time-of-flight mass spectrometer analysis (QTOF-MS). The mass spectrometer was operated in positive ion mode, with the mass range set as 300–2,000 m/z. The two most intensely electrized peptides above 20 counts were selected for tandem mass spectrometry at a dynamic exclusion for 30 s with a tolerance of ±50 mDa.

MS analysis data were processed by ProteinPilot software version 2.0 (Applied Biosystems) and compared to a human protein database International Protein Index (IPI) (v3.77). Cysteine modified by methane thiosulfate (MMTS) was specified as a fixed modification. Relative quantification of proteins was determined using ratios of the peak areas at 117, 118, 119, and 121 Da, respectively. These values corresponded to the abundances of the tags applied to label the samples.

QUANTITATIVE PCR ANALYSIS

Total RNAs were extracted from NPC tissues and the adjacent non-tumor tissues using TRIzol reagent (Ambion, Carlsbad, CA) following the manufacturer's protocol. Total RNAs were immediately reverse-transcribed into first-strand cDNA with ReverTra Ace qPCR RT kit (Toyobo, Osaka, Japan). PCR was performed using TaqMan GeneExpression Assay Kit and primers for 18S (Hs99999901_s1), GSTP1 (Hs02512067_s1), KRT5 (Hs00361185_m1), HIST2H2AC (Hs00543838_ s1), GPI (Hs00976711_m1), NPM1 (Hs02339479_g1), HSPB1 (Hs03044127_g1), MIF (Hs00236988_g1), PASP (Hs01551096_m1), YWHAE (Hs00356749_g1), LDHA (Hs00855332_g1), NCL (Hs01066668_m1), SERPINB3 (Hs00199468_m1), COL3A1 (Hs00943809_m1), RNASE3 (Hs01923184_s1), AGR2 (Hs00356521_m1), COL1A1 (Hs00164004_m1), TPSAB1 (Hs02576518_gH), COL1A2 (Hs00164099_m1), TGM2 (Hs00190278_m1). Real-time quantitative RT-PCR was performed on the ABI 7900HT System, and the results were analyzed by the $2^{-\Delta\Delta CT}$

method [Livak and Schmittgen, 2001; Schmittgen and Livak, 2008]. All experiments were performed in triplicate.

WESTERN BLOT ANALYSIS

Protein samples were extracted from the cells or clinical tissues using lysis buffer containing 100 mM NaCl, 50 mM Tris base, 1 mM $MgCl_2$, 0.5% Nonidet P-40, 0.5% Triton X-100, 1 mM PMSF, and protease inhibitors leupeptin and pepstatin A. Each protein sample was quantified with the 2-D Quant Kit. Equal amounts of protein samples were separated on SDS–PAGE gels, and then transferred onto PVDF membranes. The membranes were blocked at 4°C overnight, then incubated with primary antibodies for 3 h. The membranes were then washed in TBS-Tween solution (TBS-T) three times, and incubated with 1:5,000 diluted HPR-conjugated secondary antibody at room temperature for 1 h. Finally, the membranes were detected with the ChemiDoc^{TM} MP imaging system (Bio-Rad, Hercules, CA).

TISSUE MICROARRAY

Tissue microarrays (TMA) containing 44 NPC tissues and 56 non-tumor nasopharyngeal tissues were purchased from Biomax, Inc. (Rockville, MD). Immunohistochemistry (IHC) was performed using routine methods. Paraffin-embedded human nasopharynx tissue sections were deparaffinized, rehydrated, and antigen retrieval was performed with 0.01 M (sodium?) citrate for 5 min. Endogenous peroxidase activity was quenched in 3% H_2O_2 for 10 min. Tissue sections were then blocked with bovine serum albumin (BSA), and incubated with specific monoclonal antibodies for HSPB1 (1:200), NPM1 (1:200), and NCL (1:200). The reactions were visualized using diaminobenzidine solution (DAB) and counterstained with hematoxylin, and evaluated under a light microscope. Protein expression level was semi-quantitatively analyzed based on the percentage of positive cells ranging from 0% to 100% and the staining intensity counted as 0, 1, 2, or 3. The arithmetic product of the two parameters was reported as IHC score value. All evaluations were performed by the same qualified pathologist.

IN VITRO INVASION AND WOUND HEALING ASSAY

Three siRNA duplexes against human NPM1 (SR303222A, SR303222B, and SR303222C; OriGene Technologies) and negative control siRNA high GC duplex (Invitrogen) were transfected into CNE1 cells using Lipofectamine 2000. Approximately 48 h after transfection, the efficiency of RNA interference was confirmed by Western blot analysis, and the cells were collected for the invasion and migration array. For invasion assay, 1×10^5 siRNA-treated cells were seeded to the upper 8 μm pore size polycarbonate membrane chambers in a 24-well plate, while the bottom chambers were covered with 10% FBS medium. Non-invasive cells in the upper layer were excluded, whereas infiltrated cells in the bottom layer were dissociated, lysed and quantified by the optical density (OD) value at the wavelength of 560 nm. For wound healing assay, siRNA treated cells were seeded onto a six-well plate, and a wound was scratched on confluent monolayer perpendicular to the datum lines using pipette tips. Next the cells were washed with culture medium to remove cell debris, and cultured with fresh medium in 5%-CO_2 incubator at 37°C. Images of the scratch were captured at 0 and 24 h using a phase-contrast microscope. The relative scratch width was measured quantitatively using Adobe Photoshop CS5. Cell migration was measured as the extent of closure of the scratch gap. All experiments were performed in triplicate.

STATISTICAL ANALYSIS

Data were statistically analyzed using SPSS Statistics Client, version 20.0 (SPSS, Inc., Chicago, IL). The continuous variables were expressed as mean ± standard deviation (SD). Significant test for the intergroup variables were analyzed with the Student's *t*-test with $P < 0.05$ considered statistically significant.

RESULTS

iTRAQ METHOD PROTEOMIC ANALYSIS

Protein samples were extracted from NPC tissue or the adjacent non-tumor tissues, and labeled with the isobaric tags. Pooled peptides bonding with iTRAQ tags were profiled by tandem mass spectrometry to analyze proteins differentially expressed between NPC tissues and the adjacent non-tumor tissues (Fig. 1A). Samples were labeled in duplicate to increase reliability. The final ratios of 118:117 and 121:119 indicated the relative abundance of the proteins in NPC tissue compared to the adjacent non-tumor tissue.

Protein threshold was set to 1.3, to attain a confidence of 95% at 5% false discovery rate (FDR) (Supplementary Information 2). Using ProteinPilot 2.0 software, we identified 562 unique proteins (Supplementary Information 3, 4) based on the IPI database (version 3.77, November 2010, 89,422 sequences). Since overall technical variation was estimated below 30%, we classified potentially differentially expressed proteins with a 1.3-fold cut-off ratio. Therefore, ranges of down-regulation and up-regulation were limited as 0.77 (1/1.3) and 1.3 (1×1.3), respectively [Yang et al., 2012]. Based on the screening strategy, 54 proteins were selected as potentially differentially expressed. Of those, 25 proteins were up-regulated in NPC tissue, and the other 29 proteins were down-regulated in NPC tissue, compared to the adjacent non-tumor tissue (Table I). GSTP1 protein was the most significant among all up-regulated proteins, and its relative abundance in NPC tissues compared with the adjacent non-tumor tissues was indicated by the ratio of 118:117 and 121:119 (Fig. 1B).

CLASSIFICATION OF PROTEINS

PANTHER (http://www.pantherdb.org) was utilized to classify the 54 identified proteins according to their molecular functions and biological processes. The 54 differentially expressed proteins were represented as seven molecular function categories and 10 biological processes (Fig. 2). Binding (28.8%), catalytic activity (25.4%) and enzyme regulator activity (10.2%) ranked the first three on the molecular function categories. About a quarter of the dysregulated proteins were involved in metabolic process (26.5%). Besides, some differentially expressed proteins participated in cellular process (16.7%) and biological regulation (10.8%).

VALIDATION OF DIFFERENTIAL EXPRESSION PROTEINS

RT-PCR and Western blot analysis were performed to evaluate expression of the identified proteins. The mRNAs of SERPINB3, COL3A1, RNASE3, AGR2, COL1A1, TPSAB1, COL1A2, and TGM2 were down-regulated, while GSTP1, KRT5, HIST2H2AC, GPI, NPM1, HSPB1, MIF, PASP, YWHAE, LDHA, and NCL were up-regulated in NPC tissues, compared with the non-tumor tissues. Expression

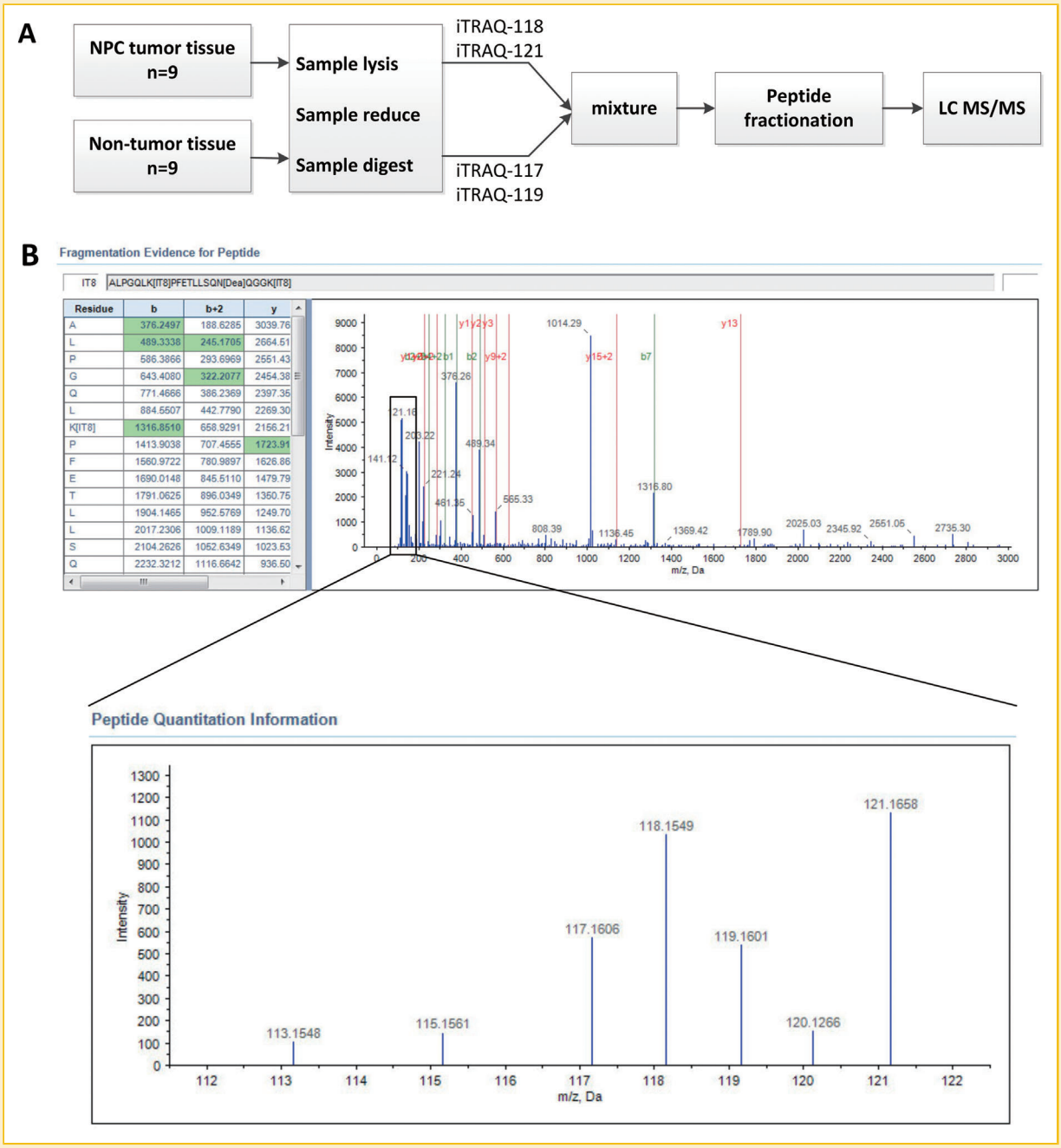

Fig. 1. A: Flow chart of iTRAQ proteomics approach. B: Representative MS/MS spectrum showing the peptides from GSTP1 (peptide sequence: ALPGQLKPFETLLSQNQGGK). NPC tissues were labeled with iTRAQ 118 and 121 tags, and non-tumor nasopharyngeal tissues were labeled with iTRAQ 117 and 119 tags. Therefore, the ratio of 118:117 and 121:119 indicated the relative abundance of GSTP1 protein in NPC tissues compared with non-tumor tissues.

patterns of these mRNAs coincided with their corresponding protein levels shown in the iTRAQ approach. Western blot analysis showed that compared with non-tumor tissues, NPC tissues had remarkably elevated levels of NPM1, NCL, and HSPB1, and down-regulation of AGR2 (Fig. 3B).

VALIDATION OF HSPB1, NPM1, AND NCL EXPRESSION BY IHC

To confirm the clinical relevance of the identified proteins, tissue microarrays containing 44 NPC tissues and 56 non-tumor nasopharyngeal tissues were applied to examine the expression of HSPB1, NPM1, and NCL in clinical tissue samples by IHC. Representative images of HSPB1, NPM1, and NCL staining in these tissues are shown in Figure 4A. HSPB1, NPM1, and NCL staining scores were higher in NPC tissues than in adjacent non-tumor tissues ($P < 0.01$). Specifically, 70/74 (94.59%) cases of NPC expressed NPM1 with IHC score >0, compared to 11/26 (42.31%) cases expressing NPM1 in non-tumor nasopharyngeal tissues. Moreover, NPM1 staining intensity was obviously stronger in TMA points of

TABLE I. Fifty-Four Proteins Identified to be Differentially Expressed Between NPC Tissues and Non-Tumor Nasopharyngeal Epithelia Tissues by iTRAQ

No.	Accession	Gene sym	Name	Unique iTRAQ peptide	118:117	*P*-Value (118:117)	121:119	*P*-Value (121:119)	Average fold change
Proteins down-regulated in NPC tumor tissues									
1	IPI:IPI00021033.2	COL3A1	Isoform 1 of Collagen alpha-1(III) chain	17	0.29	2.09E−09	0.31	6.24E−11	0.30
2	IPI:IPI00007427.2	AGR2	AGR2	3	0.33	1.83E−02	0.35	1.84E−02	0.34
3	IPI:IPI00297646.4	COL1A1	Collagen alpha-1(I) chain	59	0.36	2.76E−22	0.37	6.27E−26	0.37
4	IPI:IPI00304962.3	COL1A2	Collagen alpha-2(I) chain	47	0.39	8.68E−13	0.41	1.23E−13	0.40
5	IPI:IPI00294578.1	TGM2	Isoform 1 of protein-glutamine gamma-glutamyltransferase 2	3	0.40	4.30E−04	0.41	9.09E−04	0.40
6	IPI:IPI00215983.3	CA1	Carbonic anhydrase 1	7	0.40	2.10E−04	0.40	2.27E−04	0.40
7	IPI:IPI00218914.5	ALDH1A1	Retinal dehydrogenase 1	2	0.42	7.17E−05	0.44	3.99E−05	0.43
8	IPI:IPI00306413.3	TPPP3	Tubulin polymerization-promoting protein family member 3	3	0.45	1.78E−02	0.42	4.73E−02	0.43
9	IPI:IPI00020986.2	LUM	Lumican	2	0.45	1.74E−04	0.45	1.95E−04	0.45
10	IPI:IPI00025465.2	OGN	cDNA FLJ59205, highly similar to Mimecan	2	0.48	1.71E−02	0.55	1.67E−02	0.51
11	IPI:IPI00930684.1	IGHG3	Putative uncharacterized protein	14	0.48	9.51E−03	0.45	6.31E−04	0.47
12	IPI:IPI00386879.1	IGHA1	cDNA FLJ14473 fis, clone MAMMA1001080, highly similar to Homo sapiens SNC73 protein (SNC73) mRNA	6	0.54	8.72E−04	0.55	2.57E−03	0.55
13	IPI:IPI00654755.3	HBB	Hemoglobin subunit beta	209	0.56	3.61E−16	0.58	2.77E−12	0.57
14	IPI:IPI00171438.2	TXNDC5	Thioredoxin domain-containing protein 5	2	0.57	6.36E−03	0.61	1.24E−02	0.59
15	IPI:IPI00410714.5	HBA1	Hemoglobin subunit alpha	105	0.57	3.07E−39	0.57	7.62E−41	0.57
16	IPI:IPI00940952.1	IGKC	Ig kappa chain C region	18	0.58	3.04E−16	0.58	1.66E−15	0.58
17	IPI:IPI00903084.1	BGN	cDNA FLJ35704 fis, clone SPLEN2020183, highly similar to Biglycan	4	0.59	1.50E−02	0.58	2.03E−02	0.58
18	IPI:IPI00884926.1	ORM1	Orosomucoid 1 precursor	3	0.60	8.00E−06	0.54	9.69E−06	0.57
19	IPI:IPI00009342.1	IQGAP1	Ras GTPase-activating-like protein IQGAP1	4	0.62	1.30E−04	0.61	2.37E−03	0.62
20	IPI:IPI00553177.1	SERPINA1	Isoform 1 of alpha-1-antitrypsin	10	0.64	3.17E−04	0.59	2.56E−06	0.62
21	IPI:IPI00003817.3	ARHGDIB	Rho GDP-dissociation inhibitor 2	2	0.65	2.60E−02	0.58	4.28E−02	0.62
22	IPI:IPI00453473.6	HIST2H4B	Histone H4	25	0.65	1.42E−07	0.64	7.79E−08	0.65
23	IPI:IPI00217465.5	HIST1H1C	Histone H1.2	18	0.66	4.35E−03	0.66	8.72E−03	0.66
24	IPI:IPI00792011.1	CAPS	Calcyphosin	6	0.68	2.59E−03	0.62	4.83E−02	0.65
25	IPI:IPI00217466.3	HIST1H1D	Histone H1.3	7	0.69	2.47E−05	0.71	4.73E−04	0.70
26	IPI:IPI00021828.1	CSTB	Cystatin-B	2	0.71	1.06E−03	0.71	5.67E−04	0.71
27	IPI:IPI00745872.2	ALB	Isoform 1 of serum albumin	123	0.72	2.43E−04	0.66	3.30E−06	0.69
28	IPI:IPI00218918.5	ANXA1	Annexin A1	9	0.75	8.53E−03	0.74	4.98E−03	0.75
29	IPI:IPI00418471.6	VIM	Vimentin	80	0.76	3.39E−14	0.74	6.91E−17	0.75
Proteins up-regulated in NPC tumor tissues									
1	IPI:IPI00219757.13	GSTP1	Glutathione S-transferase P	15	2.46	7.14E−04	2.30	1.32E−03	2.38
2	IPI:IPI00009867.3	KRT5	Keratin, type II cytoskeletal 5	49	2.14	4.89E−11	2.09	2.61E−11	2.11
3	IPI:IPI00916955.1	PTMA	Putative uncharacterized protein PTMA	4	1.92	4.19E−03	1.89	4.84E−04	1.91
4	IPI:IPI00658013.1	NPM1	Nucleophosmin 1 isoform 3	4	1.82	4.42E−03	1.79	4.96E−03	1.81
5	IPI:IPI00025512.2	HSPB1	Heat shock protein beta-1	12	1.80	2.45E−06	1.83	1.62E−06	1.82
6	IPI:IPI00293276.10	MIF	Macrophage migration inhibitory factor	3	1.80	3.97E−03	1.82	8.90E−03	1.81
7	IPI:IPI00943181.1	PSME2	Putative uncharacterized protein PSME2	6	1.79	2.27E−02	1.82	1.91E−02	1.80
8	IPI:IPI00220362.5	HSPE1	10 kDa heat shock protein, mitochondrial	2	1.77	1.38E−04	1.81	1.13E−04	1.79
9	IPI:IPI00947127.1	LDHA	Lactate dehydrogenase A isoform 3	10	1.75	6.10E−03	1.66	9.01E−03	1.71
10	IPI:IPI00414676.6	HSP90AB1	Heat shock protein HSP 90-beta	11	1.71	2.26E−04	1.73	2.73E−04	1.72
11	IPI:IPI00939370.1	CKAP4	CKAP4 protein (fragment)	3	1.70	1.25E−03	1.75	1.08E−03	1.72
12	IPI:IPI00794461.1	HIST1H2BN	Histone H2B type 1-N	44	1.67	5.79E−03	1.60	1.55E−02	1.64
13	IPI:IPI00792352.1	RANP1	26 kDa protein	4	1.65	1.64E−03	1.52	3.15E−03	1.58
14	IPI:IPI00550020.3	PTMS	Parathymosin	2	1.59	2.30E−02	1.56	2.95E−02	1.58
15	IPI:IPI00795292.1	NME2	Isoform 3 of nucleoside diphosphate kinase B	2	1.57	5.01E−03	1.62	4.33E−03	1.59
16	IPI:IPI00937615.2	EEF1G	Elongation factor 1-gamma	2	1.51	1.90E−03	1.52	2.99E−05	1.52
17	IPI:IPI00025491.1	EIF4A1	Eukaryotic initiation factor 4A-I	3	1.49	1.24E−02	1.50	4.39E−04	1.49
18	IPI:IPI00419585.9	PPIA	Peptidyl-prolyl cis-trans isomerase A	18	1.48	6.59E−05	1.52	7.97E−05	1.50
19	IPI:IPI00396485.3	EEF1A1	Elongation factor 1-alpha 1	17	1.48	5.17E−03	1.48	2.09E−03	1.48
20	IPI:IPI00465248.5	ENO1	Isoform alpha-enolase of alpha-enolase	25	1.47	1.14E−05	1.49	4.20E−07	1.48
21	IPI:IPI00021263.3	YWHAZ	14-3-3 protein zeta/delta	7	1.43	1.76E−02	1.52	1.68E−03	1.47
22	IPI:IPI00465028.7	TPI1	Triosephosphate isomerase 1 isoform 2	14	1.42	2.82E−04	1.35	4.33E−04	1.38
23	IPI:IPI00032140.4	SERPINH1	Serpin H1	5	1.42	1.92E−02	1.49	1.15E−03	1.46
24	IPI:IPI00645201.1	RPS8	Ribosomal protein S8	2	1.40	1.11E−02	1.31	3.14E−02	1.36
25	IPI:IPI00784154.1	HSPD1	60 kDa heat shock protein, mitochondrial	30	1.34	4.05E−04	1.37	1.92E−03	1.35

iTRAQ tags assignment: NPC tumor tissue: −118 and −121; non-tumor tissue: −117 and −119
Statistical analysis for iTRAQ-based detection and relative quantification was performed using the Paragon Algorithm in the ProteinPilot™ software.

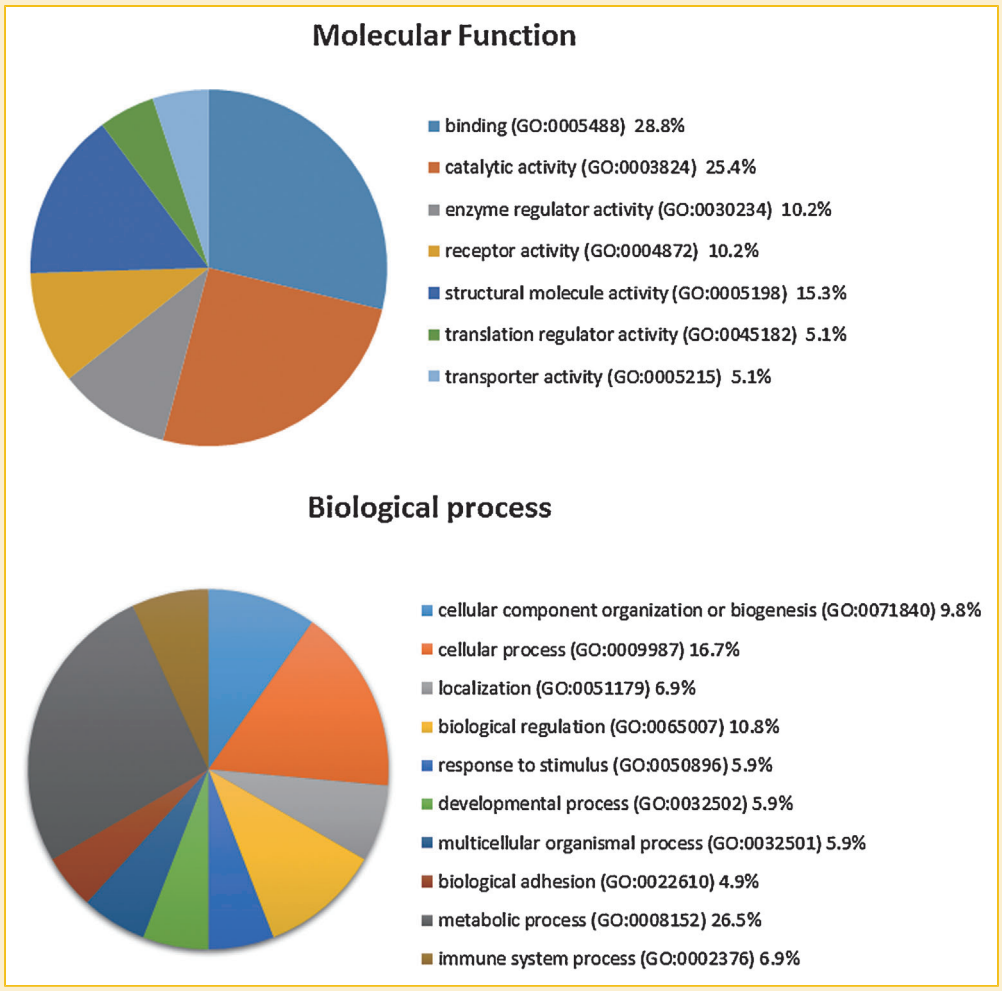

Fig. 2. The categories of 54 differentially expressed proteins grouped by molecular function and biological process using PANTHER system.

NPC than those points of non-tumor nasopharyngeal tissue. Similar results were observed for HSPB1 and NCL protein (Fig. 4B). These data are consistent with the results of RT-PCR and Western blot analysis.

NPM1 REGULATES THE INVASION AND MIGRATION OF NPC CELLS

NPM1 protein expression in CNE1 cells was effectively silenced by NPM1-specific siRNA compared to the control group (Fig. 5A). Cell invasion assay showed significant inhibition of cell invasion in cells transfected with NPM1-specific siRNAs compared to those transfected with negative control siRNA (Fig. 5B). In the wound healing assay, cells transfected with NPM1-specific siRNAs had inhibited migration compared to those transfected with negative control siRNA (Fig. 5C). These results indicated that NPM1 regulates the invasion and migration of NPC cells.

DISCUSSION

NPC is the most common type of head and neck tumor in southern China [Yu and Yuan, 2002]. Because of the hidden anatomical location and non-specific symptoms, definitive diagnosis of NPC relies on endoscopic biopsy. Nevertheless, histopathology is not a feasible choice for tumor screening or early detection. Because EBV is a high risk factor of NPC, EBV antibodies are widely used as screening and diagnostic markers for NPC, but they lack specificity [Altun et al., 1995]. Quantitative proteomics is a useful tool to identify disease markers, especially isotope-based quantitative proteomics. Previous proteomic studies were mostly conducted using the 2-DE approach. By a quantitative proteome analysis based on 2D-DIGE, 14-3-3-γ was found up-regulated in Cripto-1 overexpressed CNE1 cells and as a potential biomarker of NPC [Wu et al., 2013]. Since the utilization of 2-DE is limited in many aspects, iTRAQ is emerging as a high-throughput isotope-based quantitative proteomics approach [Guo et al., 2008; Tong et al., 2012]. A previous study analyzed the proteomic profile of formalin-fixed and paraffin-embedded NPC tissues, which identified that cathepsin D, keratin8, SFN, and stathmin1 were significantly dysregulated [Xiao et al., 2010]. In our study, 54 differentially expressed proteins were identified from fresh-frozen NPC tissues and the adjacent non-tumor tissues in the iTRAQ proteomic approach. These proteins were classified based on their molecular function and biological process, respectively. Most of the differentially expressed proteins have binding and catalytic

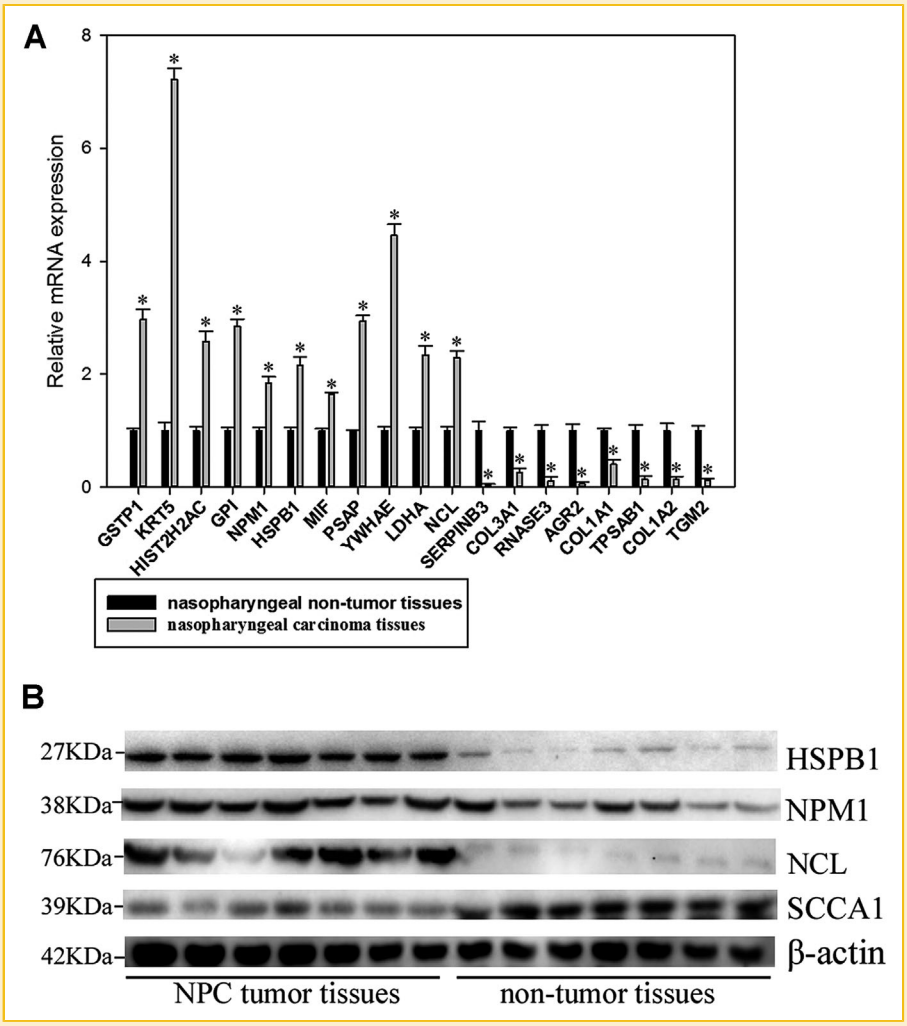

Fig. 3. Evaluation of the potentially differentially expressed proteins in NPC tissues and normal nasopharyngeal tissues. A: Real-time PCR analysis of the relative mRNA levels of GSTP1, KRT5, HIST2H2AC, GPI, NPM1, HSPB1, MIF, PSAP, YWHAE, LDHA, NCL, SERPINB3, COL3A1, RNASE3, AGR2, COL1A1, TPSAB1, COL1A2, and TGM2. 18S rRNA was used as the normalization standard. Compared with normal tissues, NPC tissues had up-regulation of GSTP1, KRT5, HIST2H2AC, GPI, NPM1, HSPB1, MIF, PSAP, YWHAE, LDHA, and NCL, and down-regulation of SERPINB3, COL3A1, RNASE3, AGR2, COL1A1, TPSAB1, COL1A2, and TGM2. $^{*}P < 0.05$ versus control by *t*-test. B: Representative Western blot analysis of HSPB1, NCL, NPM1, and SCCA1 expression in NPC tissues and normal nasopharyngeal tissues. Compared with normal tissue, NPC had up-regulation of HSPB1, NCL and NPM1, and down-regulation of SCCA1.

activities that are associated with the biological processes in which they participated such as metabolic process, cellular process and biological regulation. Among these, we confirmed the differential expression of GSTP1, KRT5, HIST2H2AC, GPI, NPM1, HSPB1, MIF, PASP, YWHAE, LDHA, HSP90AB1, SERPINB3, COL3A1, RNASE3, AGR2, COL1A1, TPSAB1, COL1A2, and TGM2 by RT-PCR and Western blot analysis. Furthermore, the differential expression of HSPB1, NPM1, and NCL were validated by IHC of tissue microarrays of 44 NPC tissues and 56 non-tumor nasopharyngeal tissues. The results of RT-PCR, Western blot and IHC are consistent with the results of iTRAQ, supporting that iTRAQ analysis is reliable and efficient for large-scale proteomic quantification.

The 54 differentially expressed proteins were classified into 10 categories according to their molecular function based on PANTHER analysis. NPM1, or nucleophosmin, is a nucleolar phosphoprotein which is highly concentrated in the nucleolar granular regions [Yung et al., 1985]. NPM1 shuttles between the nucleus and cytoplasm to regulate cellular activities such as proliferation and growth suppression [Yun et al., 2003; Grisendi et al., 2006]. In addition, NPM1 participates in series of other biological and pathological processes including centrosome duplication [Okuda et al., 2000], ribosome biogenesis [Boon et al., 2001], protein chaperone [Szebeni et al., 2003], histone assembly, cell proliferation [Feuerstein and Mond, 1987] and apoptosis [Yang et al., 2007]. NPM1 could modulate the activity and stability of tumor-suppressor p53 and is a positive regulator of the ARF tumor-suppressor pathway [Grisendi et al., 2006]. In addition, NPM1 is recognized as one of the most frequent targets of genetic alterations in hematopoietic cancers. In particular, NPM1 gene mutations have been implicated in the genesis, evolution [Dai and Ren, 2013; Noguera et al., 2013; Rodriguez-Macias et al.,

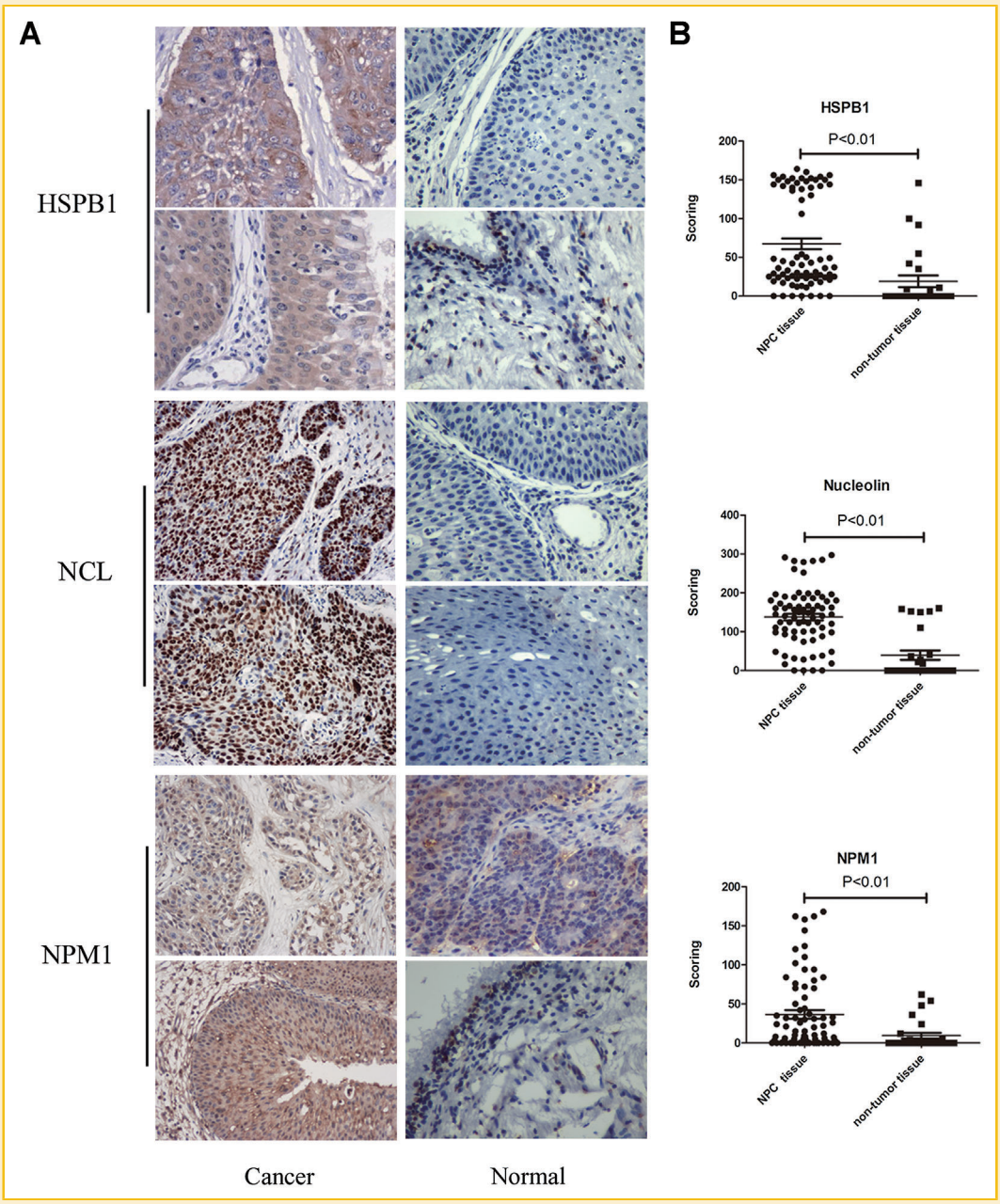

Fig. 4. Validation of HSPB1, NCL, and NPM1 overexpression in NPC tissues by tissue microarrays. A: Representative images of ICH staining of HSPB1, NCL, and NPM1 in NPC tissues and normal nasopharyngeal tissues. B: IHC score values of HSPB1, NCL, and NPM1 were higher in NPC tissues than in normal tissues.

2013], relapse [Kronke et al., 2013], death evasion and drug sensitivity of acute myeloid leukemia (AML) [Lo et al., 2013]. On the other hand, NPM1 is ubiquitously overexpressed in solid tumors including gastric cancer [Tanaka et al., 1992; Yang et al., 2007], colon cancer [Liu et al., 2012; Wong et al., 2013], prostate cancer [Tsui et al., 2004], ovarian cancer [Shields et al., 1997], endometrial cancer [Chao et al., 2013], and breast cancer [Skaar et al., 1998]. In this study, we found that NPM1 was up-regulated in NPC tissues compared to adjacent non-tumor nasopharyngeal tissues. Tissue microarrays verified that NPM1 expression was significantly higher in clinical NPC samples than in non-tumor nasopharyngeal tissues, implying that NPM1 might be a potentially promising candidate biomarker of NPC. Furthermore, siRNA mediated knockdown of NPM1 significantly decreased invasion and migration ability of CNE1 cell line, confirming that NPM1 may be a novel target for anti-cancer therapy of NPC.

Heat shock protein beta-1 (HSPB1) was remarkably up-regulated in NPC tissues, compared with nasopharyngeal non-tumor tissues. Tissue microarrays showed significant overexpression of HSPB1 in NPC tissues. HSPB1 belongs to chaperone protein superfamily [Hendrick and Hartl, 1993]. HSPB1 overexpression has been correlated with risk in lung cancer [Guo et al., 2010; Xu et al., 2012a], pancreatic cancer [Heinrich et al., 2011; Shiota et al., 2013],

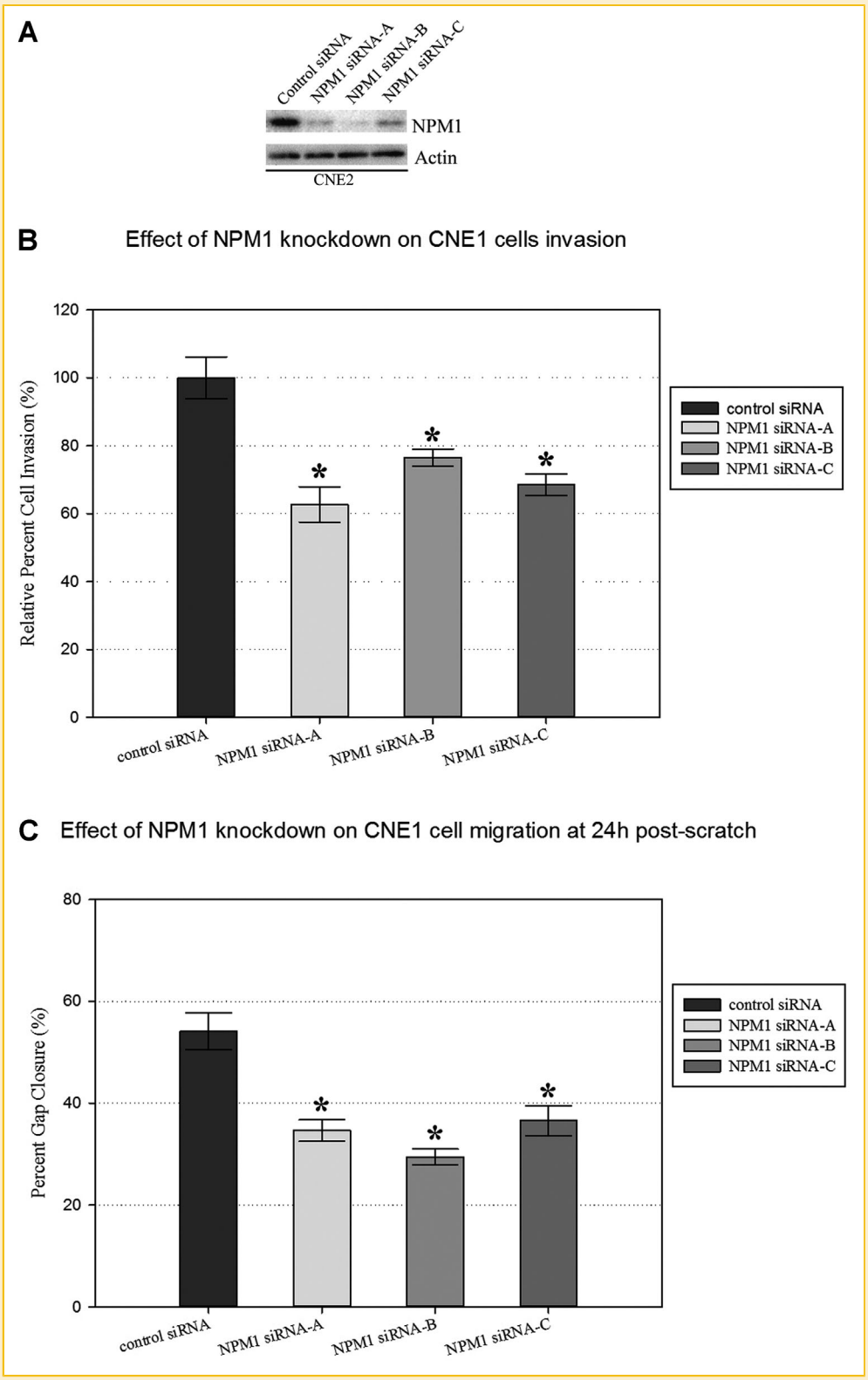

Fig. 5. NPM1 regulates NPC cell invasion and migration. A: Western blot analysis of NPM1 protein level in CNE1 cells transfected with three NPM1-specific siRNA or control siRNA. B: Silencing of NPM1 significantly inhibited the invasion of CNE1 cells. C: Silencing of NPM1 led to the reduction in the ability of CNE1 cell line to close the gap introduced by a scratch wound.

prostate cancer [Shiota et al., 2013] and ovarian cancer [Zhao et al., 2012], and is involved in interferon pathway activation in HBV-associated hepatocellular carcinoma [Tong et al., 2013]. Several studies have demonstrated that HSPB1 is a chemoradiation-related protein which may promote drug-resistance and radioresistance in cancer therapy [Zhang et al., 2012; Xu et al., 2012a; Pang et al., 2013]. Therefore, HSPB1 may also play a vital role in the genesis and progression of NPC.

Nucleolin (NCL) was also remarkably up-regulated in NPC tissues. NCL is an abundant, ubiquitously expressed nucleolar protein that is also found in various cellular components [Mongelard and Bouvet, 2007]. NCL participates in RNA regulatory mechanisms such as mRNA stability, transcription, translation, ribosome assembly, and microRNA processing [Abdelmohsen and Gorospe, 2012], thereby enabling cells to become malignant, for example by promoting growth and proliferation, overcoming senescence, and evading apoptosis [Dunn et al., 2004; Hanahan and Weinberg, 2011]. NCL protein is related to oncogenesis of gliomas and breast cancer [Destouches et al., 2008; Xu et al., 2012b]. Considering these results, NCL may play a crucial part in NPC and is a candidate biomarker for early diagnosis and prognosis of NPC.

In addition, several proteins identified in this study have been implicated in NPC progression. These proteins include KRT5, SERPINB3 (SCCA1), and AGR2. SCCA1 is a protease inhibitor that modulates the host immune response against tumor cells and regulates apoptotic pathways [Vidalino et al., 2009]. Down-regulation of SCCA1 protein in NPC tissues may lead to the inhibition of tumor cell apoptosis, resulting in tumor cell proliferation. The in-depth mechanism of SCCA1 in NPC will be the focus of our future studies.

NPC remains a high-mortality malignant carcinoma among head and neck cancers, especially in southern China. Therefore, it is urgent to identify novel biomarkers for improved diagnosis and treatments of NPC. In this study, we used the iTRAQ method to identify 54 differentially expressed proteins in NPC tissues, such as NPM1, HSPB1, NCL, and SCCA1. These proteins are potential targets for the diagnosis and therapy of NPC.

REFERENCES

Abdelmohsen K, Gorospe M. 2012. RNA-binding protein nucleolin in disease. RNA Biol 9:799–808.

Altun M, Fandi A, Dupuis O, Cvitkovic E, Krajina Z, Eschwege F. 1995. Undifferentiated nasopharyngeal cancer (UCNT): Current diagnostic and therapeutic aspects. Int J Radiat Oncol Biol Phys 32:859–877.

Anghel I, Anghel AG, Dumitru MCCS. 2012. Nasopharyngeal carcinoma—Analysis of risk factors and immunological markers. Chirurgia (Bucur).

Boon K, Caron HN, van Asperen R, Valentijn L, Hermus MC, van Sluis P, Roobeek I, Weis I, Voute PA, Schwab M, Versteeg R. 2001. N-myc enhances the expression of a large set of genes functioning in ribosome biogenesis and protein synthesis. EMBO J 20:1383–1393.

Cao SMLZ, Jia WH, Huang QH, Liu Q, Guo X, Huang TB, Ye W, Hong MH. 2011. Fluctuations of Epstein–Barr virus serological antibodies and risk for nasopharyngeal carcinoma: A prospective screening study with a 20-year follow-up. PLoS ONE.

Chan KC, Hung EC, Woo JK, Chan PK, Leung SF, Lai FP, Cheng AS, Yeung SW, Chan YW, Tsui TK, Kwok JS, King AD, Chan AT, van Hasselt AC, Lo YM. 2013. Early detection of nasopharyngeal carcinoma by plasma Epstein–Barr virus DNA analysis in a surveillance program. Cancer 119:1838–1844.

Chao A, Lin CY, Tsai CL, Hsueh S, Lin YY, Lin CT, Chou HH, Wang TH, Lai CH, Wang HS. 2013. Estrogen stimulates the proliferation of human endometrial cancer cells by stabilizing nucleophosmin/B23 (NPM/B23). J Mol Med (Berl) 91:249–259.

Dai Q, Ren Y. 2013. Cytoplasmic expression of nucleophosmin 1 as a marker for diagnosing residual disease of acute myeloid leukemia. Appl Immunohistochem Mol Morphol 21:205–211.

Destouches D, El Khoury D, Hamma-Kourbali Y, Krust B, Albanese P, Katsoris P, Guichard G, Briand JP, Courty J, Hovanessian AG. 2008. Suppression of tumor growth and angiogenesis by a specific antagonist of the cell-surface expressed nucleolin. PLoS ONE 3:e2518.

Dunn GP, Old LJ, Schreiber RD. 2004. The immunobiology of cancer immunosurveillance and immunoediting. Immunity 21:137–148.

Feinmesser R, Miyazaki I, Cheung R, Freeman JL, Noyek AM, Dosch HM. 1992. Diagnosis of nasopharyngeal carcinoma by DNA amplification of tissue obtained by fine-needle aspiration. N Engl J Med 326:17–21.

Feng XP, Yi H, Li MY, Li XH, Yi B, Zhang PF, Li C, Peng F, Tang CE, Li JL, Chen ZC, Xiao ZQ. 2010. Identification of biomarkers for predicting nasopharyngeal carcinoma response to radiotherapy by proteomics. Cancer Res 70:3450–3462.

Feuerstein N, Mond JJ. 1987. Identification of a prominent nuclear protein associated with proliferation of normal and malignant B cells. J Immunol 139:1818–1822.

Gorg A, Obermaier C, Boguth G, Harder A, Scheibe B, Wildgruber R, Weiss W. 2000. The current state of two-dimensional electrophoresis with immobilized pH gradients. Electrophoresis 21:1037–1053.

Gorg A, Weiss W, Dunn MJ. 2004. Current two-dimensional electrophoresis technology for proteomics. Proteomics 4:3665–3685.

Grisendi S, Mecucci C, Falini B, Pandolfi PP. 2006. Nucleophosmin and cancer. Nat Rev Cancer 6:493–505.

Guo H, Bai Y, Xu P, Hu Z, Liu L, Wang F, Jin G, Wang F, Deng Q, Tu Y, Feng M, Lu D, Shen H, Wu T. 2010. Functional promoter -1271G>C variant of HSPB1 predicts lung cancer risk and survival. J Clin Oncol 28:1928–1935.

Guo T, Gan CS, Zhang H, Zhu Y, Kon OL, Sze SK. 2008. Hybridization of pulsed-Q dissociation and collision-activated dissociation in linear ion trap mass spectrometer for iTRAQ quantitation. J Proteome Res 7:4831–4840.

Hanahan D, Weinberg RA. 2011. Hallmarks of cancer: The next generation. Cell 144:646–674.

Hendrick JP, Hartl FU. 1993. Molecular chaperone functions of heat-shock proteins. Annu Rev Biochem 62:349–384.

Heinrich JC, Tuukkanen A, Schroeder M, Fahrig T, Fahrig R. 2011. RP101 (brivudine) binds to heat shock protein HSP27 (HSPB1) and enhances survival in animals and pancreatic cancer patients. J Cancer Res Clin Oncol 137:1349–1361.

Kronke J, Bullinger L, Teleanu V, Tschurtz F, Gaidzik VI, Kuhn MW, Rucker FG, Holzmann K, Paschka P, Kapp-Schworer S, Spath D, Kindler T, Schittenhelm M, Krauter J, Ganser A, Gohring G, Schlegelberger B, Schlenk RF, Dohner H, Dohner K. 2013. Clonal evolution in relapsed NPM1-mutated acute myeloid leukemia. Blood 122:100–108.

Liu Y, Cai H, Liu J, Fan H, Wang Z, Wang Q, Shao M, Sun X, Diao J, Liu Y, Shi Y, Fan Q. 2013. A miR-151 binding site polymorphism in the 3′-untranslated region of the cyclin E1 gene associated with nasopharyngeal carcinoma. Biochem Biophys Res Commun 432:660–665.

Liu Y, Zhang F, Zhang XF, Qi LS, Yang L, Guo H, Zhang N. 2012. Expression of nucleophosmin/NPM1 correlates with migration and invasiveness of colon cancer cells. J Biomed Sci 19:53.

Livak KJ, Schmittgen TD. 2001. Analysis of relative gene expression data using real-time quantitative PCR and the 2(−Delta Delta C(T)) Method. Methods 25:402–448.

Lo SJ, Fan LC, Tsai YF, Lin KY, Huang HL, Wang TH, Liu H, Chen TC, Huang SF, Chang CJ, Lin YJ, Yung BY, Hsieh SY. 2013. A novel interaction of nucleophosmin with BCL2-associated X protein regulating death evasion and drug sensitivity in human hepatoma cells. Hepatology 57:1893–1905.

Mirgorodskaya OA, Kozmin YP, Titov MI, Körner R, Sönksen CPPR. 2000. Quantitation of peptides and proteins by matrix-assisted laser desorption-ionization mass spectrometry using (18)O-labeled internal standards. Rapid Commun Mass Spectrom.

Mongelard F, Bouvet P. 2007. Nucleolin: A multiFACeTed protein. Trends Cell Biol 17:80–86.

Noguera NI, Song MS, Divona M, Catalano G, Calvo KL, Garcia F, Ottone T, Florenzano F, Faraoni I, Battistini L, Colombo E, Amadori S, Pandolfi PP, Lo-Coco F. 2013. Nucleophosmin/B26 regulates PTEN through interaction with HAUSP in acute myeloid leukemia. Leukemia 27:1037–1043.

Okuda M, Horn HF, Tarapore P, Tokuyama Y, Smulian AG, Chan PK, Knudsen ES, Hofmann IA, Snyder JD, Bove KE, Fukasawa K. 2000. Nucleophosmin/B23 is a target of CDK2/cyclin E in centrosome duplication. Cell 103:127–140.

Pang Q, Wei Q, Xu T, Yuan X, Lopez Guerra JL, Levy LB, Liu Z, Gomez DR, Zhuang Y, Wang LE, Mohan R, Komaki R, Liao Z. 2013. Functional promoter variant rs2868371 of HSPB1 is associated with risk of radiation pneumonitis after chemoradiation for non-small cell lung cancer. Int J Radiat Oncol Biol Phys 85:1332–1339.

Rodriguez-Macias G, Martinez-Laperche C, Gayoso J, Noriega V, Serrano D, Balsalobre P, Munoz-Martinez C, Diez-Martin JL, Buno I. 2013. Mutation of the NPM1 gene contributes to the development of donor cell-derived acute myeloid leukemia after unrelated cord blood transplantation for acute lymphoblastic leukemia. Hum Pathol 44:1696–1699.

Schmittgen TD, Livak KJ. 2008. Analyzing real-time PCR data by the comparative CT method. Nat Protoc 3:1101–1108.

Shields LB, Gercel-Taylor C, Yashar CM, Wan TC, Katsanis WA, Spinnato JA, Taylor DD. 1997. Induction of immune responses to ovarian tumor antigens by multiparity. J Soc Gynecol Investig 4:298–304.

Shiota M, Bishop JL, Nip KM, Zardan A, Takeuchi A, Cordonnier T, Beraldi E, Bazov J, Fazli L, Chi K, Gleave M, Zoubeidi A. 2013. Hsp27 regulates epithelial mesenchymal transition, metastasis, and circulating tumor cells in prostate cancer. Cancer Res 73:3109–3119.

Skaar TC, Prasad SC, Sharareh S, Lippman ME, Brunner N, Clarke R. 1998. Two-dimensional gel electrophoresis analyses identify nucleophosmin as an estrogen regulated protein associated with acquired estrogen-independence in human breast cancer cells. J Steroid Biochem Mol Biol 67:391–402.

Szebeni A, Hingorani K, Negi S, Olson MO. 2003. Role of protein kinase CK2 phosphorylation in the molecular chaperone activity of nucleolar protein b23. J Biol Chem 278:9107–9115.

Tanaka M, Sasaki H, Kino I, Sugimura T, Terada M. 1992. Genes preferentially expressed in embryo stomach are predominantly expressed in gastric cancer. Cancer Res 52:3372–3377.

Tong SW, Yang YX, Hu HD, An X, Ye F, Hu P, Ren H, Li SL, Zhang DZ. 2012. Proteomic investigation of 5-fluorouracil resistance in a human hepatocellular carcinoma cell line. J Cell Biochem 113:1671–1680.

Tong SW, Yang YX, Hu HD, An X, Ye F, Ren H, Li SL, Zhang DZ. 2013. HSPB1 is an intracellular antiviral factor against hepatitis B virus. J Cell Biochem 114:162–173.

Tsui KH, Cheng AJ, Chang P, Pan TL, Yung BY. 2004. Association of nucleophosmin/B23 mRNA expression with clinical outcome in patients with bladder carcinoma. Urology 64:839–844.

Vidalino L, Doria A, Quarta S, Zen M, Gatta A, Pontisso P. 2009. SERPINB3, apoptosis and autoimmunity. Autoimmun Rev 9:108–112.

Wei WI, Sham JS. 2005. Nasopharyngeal carcinoma. Lancet 365:2041–2054.

Wong JC, Hasan MR, Rahman M, Yu AC, Chan SK, Schaeffer DF, Kennecke HF, Lim HJ, Owen D, Tai IT. 2013. Nucleophosmin 1, upregulated in adenomas and cancers of the colon, inhibits p53-mediated cellular senescence. Int J Cancer 133:1567–1577.

Wu Z, Weng D, Li G. 2013. Quantitative proteome analysis of overexpressed Cripto-1 tumor cell reveals 14-3-3gamma as a novel biomarker in nasopharyngeal carcinoma. J Proteomics 83:26–36.

Xiao Z, Li G, Chen Y, Li M, Peng F, Li C, Li F, Yu Y, Ouyang Y, Xiao Z, Chen Z. 2010. Quantitative proteomic analysis of formalin-fixed and paraffin-embedded nasopharyngeal carcinoma using iTRAQ labeling, two-dimensional liquid chromatography, and tandem mass spectrometry. J Histochem Cytochem 58:517–527.

Xu Z, Joshi N, Agarwal A, Dahiya S, Bittner P, Smith E, Taylor S, Piwnica-Worms D, Weber J, Leonard JR. 2012b. Knocking down nucleolin expression in gliomas inhibits tumor growth and induces cell cycle arrest. J Neurooncol 108:59–67.

Xu T, Wei Q, Lopez Guerra JL, Wang LE, Liu Z, Gomez D, O'Reilly M, Lin SH, Zhuang Y, Levy LB, Mohan R, Zhou H, Liao Z. 2012a. HSPB1 gene polymorphisms predict risk of mortality for US patients after radio(chemo)therapy for non-small cell lung cancer. Int J Radiat Oncol Biol Phys 84:e229–e235.

Yang YX, Hu HD, Zhang DZ, Ren H. 2007. Identification of proteins responsible for the development of adriamycin resistance in human gastric cancer cells using comparative proteomics analysis. J Biochem Mol Biol 40:853–860.

Yang Y, Toy W, Choong LY, Hou P, Ashktorab H, Smoot DT, Yeoh KG, Lim YP. 2012. Discovery of SLC3A2 cell membrane protein as a potential gastric cancer biomarker: Implications in molecular imaging. J Proteome Res 11:5736–5747.

Yu KJ, Hsu WL, Pfeiffer RM, Chiang CJ, Wang CP, Lou PJ, Cheng YJ, Gravitt P, Diehl SR, Goldstein AM, Chen CJ, Hildesheim A. 2011. Prognostic utility of anti-EBV antibody testing for defining NPC risk among individuals from high-risk NPC families. Clin Cancer Res 17:1906–1914.

Yu MC. 1990. Diet and nasopharyngeal carcinoma. FEMS Microbiol Immunol 2:235–242.

Yu MC, Yuan JM. 2002. Epidemiology of nasopharyngeal carcinoma. Semin Cancer Biol 12:421–429.

Yun JP, Chew EC, Liew CT, Chan JY, Jin ML, Ding MX, Fai YH, Li HK, Liang XM, Wu QL. 2003. Nucleophosmin/B23 is a proliferate shuttle protein associated with nuclear matrix. J Cell Biochem 90:1140–1148.

Yung BY, Busch H, Chan PK. 1985. Translocation of nucleolar phosphoprotein B23 (37 kDa/pI 5.1) induced by selective inhibitors of ribosome synthesis. Biochim Biophys Acta 826:167–173.

Zhang B, Qu JQ, Xiao L, Yi H, Zhang PF, Li MY, Hu R, Wan XX, He QY, Li JH, Ye X, Xiao ZQ, Feng XP. 2012. Identification of heat shock protein 27 as a radioresistance-related protein in nasopharyngeal carcinoma cells. J Cancer Res Clin Oncol 138:2117–2125.

Zhao M, Shen F, Yin YX, Yang YY, Xiang DJ, Chen Q. 2012. Increased expression of heat shock protein 27 correlates with peritoneal metastasis in epithelial ovarian cancer. Reprod Sci 19:748–753.

SUPPORTING INFORMATION

Additional Supporting Information may be found in the online version of this article at the publisher's web-site.